FACULTY OF TRANSPORT ENGINEERING 25 YEARS

VII. International Scientific Conference of the Faculty of Transport Engineering

6^{th} – 7^{th} September 2018, Pardubice

LOSS OF STABILITY OF DYNAMICALLY LOADED IDEAL CYLINDRICAL SHELL WELDED TO SADDLE SUPPORT

Ing. Dušan Mihalik[1], prof. Ing. Petr Paščenko, PhD.[2]

Abstract

The article deals with the loss of stability of a cylindrical shell at dynamic transverse load. A typical practical example of this kind of construction is a road tank welded to saddle supports. All known domestic or foreign standards or recommendations for thin-walled shell structures such as ČSN 690010 [1], EN 13445-3 [2], EN 1993-1-6 [3], AD-Merkblätt [4], DIN 18800 [5], ASMECode [6], European recommendation ECCS 2008 [7] etc., provide the solution of stability of thin-walled shell structures for static load only. However, the situation of the traffic vehicles like road tanks is more complex because, in the vast majority of cases, these are loaded dynamically. Within this article, computational FEM analysis of the dynamically loaded cylindrical shell has been applied on a geometrically reduced model, which will later be more suitable for experimental verification. The cylindrical shell is firmly attached to the single saddle support through which both static and dynamic reaction forces are transmitted. The saddle support embracing angle takes values 2φ = 60°/90°/120° in accord with the demand of the standards and recommendations mentioned above. At first, the loss of stability of the statically loaded cylindrical shell has been analysed. Both geometric and material nonlinearities have been taken into consideration. The geometric nonlinearity describes the loss of stability while material nonlinearity describes the limit state of elastic-plastic carrying capacity. The resulting phenomenon is a nonlinear stability snap-through of the saddle support into the cylindrical shell in the elastic-plastic field due to the static load. At second, the dynamic analysis of the same problem follows. The initial load velocity is selected in the range of 1 to 15 $m \cdot sec^{-1}$. The upper limit of the initial velocity corresponds to the maximum possible piston speed of the hydraulic pulsator installed at Education and Research Center in Transport (ERCT) of the Faculty of Transport Engineering, University Pardubice. The hydraulic pulsator will be used for the planned experimental testing designed based on the analysis results presented in this article. At the end of the article, the static and dynamic load capacities of the computational model have been compared and then conclusions have been made based on this outcome.

Keywords

Road tank, cylindrical shell, saddle support, linear buckling, nonlinear buckling, snap-through, static stability, dynamic stability

[1]**Ing. Dušan Mihalik**, University of Pardubice, Faculty of Transport Engineering. Educational and Research Centre in Transport, Doubravice 41, 533 53 Pardubice, Czech Republic. Phone: +420 724 760 816, E-mail: dus.mihalik@gmail.com

[2]**prof. Ing. Petr Paščenko, Ph.D.**, University of Pardubice, Faculty of Transport Engineering. Educational and Research Centre in Transport, Doubravice 41, 533 53 Pardubice, Czech Republic. Phone: +420 466 036 231, E-mail: petr.pascenko@upce.cz

1 INTRODUCTION

The shell structures are represented in the transport technology significantly. Their main advantage is low weight at relatively high rigidity and strength. The largest share of the shells used in the transportation technology is evident from the design of the self-supporting skeletons of cars or road tanks, which are subjects to this article. A typical road tank is a horizontal cylindrical shell firmly attached (usually welded) to saddle supports. The existing standards and recommendations [1 to 7] only offer the methodology and analytical formulas for stability evaluation of statically loaded shells on the saddle supports such as horizontal storage tanks and reservoirs in chemical and energy industries. The load is represented by the radial reaction force acting on the cylindrical shell from the saddle support side. In the field of transport, however, it is essential to know the behaviour of dynamically loaded road tanks. The time-varying load imitates the real load of the shell when driving a road tank on uneven terrain. **Fig.1** shows a typical example of a road tank which is attached to the truck with a saddle supports [8].

Excessive static load of the thin-walled road tank results in a snap-through of the saddle into the shell in the elastic-plastic area. Both geometric and material nonlinearity is applied. The cylindrical shell loaded with transverse force (saddle reaction) needs to be considered as a substantially geometrically nonlinear structure as the shell is thin-walled and as there is a high proportion of bending stresses in relation to the basic membrane stresses [9]. Therefore, the linear buckling analysis (LBA) suitable for elastic stability problems can only be used for basic orientation with the utmost caution.

Fig. 1 Road tank anchored on the saddle supports [8]

Even though the determination of the carrying capacity of the statically loaded cylindrical shell on the saddle supports is possible based on the standards and recommendations [1 to 7]. A comprehensive methodology for dealing with this problem for dynamic loading still has not been available. However, an increasing carrying capacity with increasing load speed can be expected. This has to be proved by following computational non-linear analyses.

2 ANALYSIS

The computational analysis of the carrying capacity of the cylindrical shell on the single saddle support of various embracing angles 2φ = 60°/90°/120° and various initial velocities v_0 =1÷15 m/sec has been performed. The weight of the model identical to the weight of the planned reduced test sample of the road tank is m_{TOT} = 8,3 kg. Neither the various saddle support width $2b$ nor the initial shape imperfections of the shell have been taken into consideration yet. All the analyses have been performed by means of the computer program SIMULATION [10].

Before the actual dynamic analysis of the computational model, several assistive computational procedures have been made. These include Linear buckling analysis (LBA), Geometric and material nonlinear analysis (GMNA) and Modal analysis (MA). The LBA provides a very rough stability estimation of the computational model in the linear field, while GMNA provides a relatively precise carrying capacity of the model in the elastic-plastic field. MA leads to the lowest significant eigenvalue necessary for the calculation of the simplified Rayleigh's damping coefficients α, β (proportional damping). The used methods are described in more detail later.

2.1 Computation model of the road tank

The computation model of the road tank on saddle supports is not in 1:1 scale, but it is diminished to allow the easier performance of the planned experiments in a laboratory. A non-dimension thin-wall *r/t* parameter is used for this purpose. For simplicity, saddle support fixed at the base is not equipped with backing plates (in the shell-saddle joint) as a real road tank. The basic input parameters of the computational model are listed in **Tab. 1**.

Tab. 1 Basic input parameters of the computational model

Length of the cylindrical shell *L*	[mm]	300
Radius of the shell *r*	[mm]	75
Thickness of the cylindrical shell *t*	[mm]	0,55
Thickness of the end t_f	[mm]	30
Width of the saddle support *2b*	[mm]	20
Embracing angle of the saddle support 2φ	[°]	60,90,120
Material of the calculation model	[-]	P235GH
Yield stress at the room temperature $R_{p0,2}$ [11]	[MPa]	235
Total weight of the calculation model m_{TOT}	[kg]	8,3

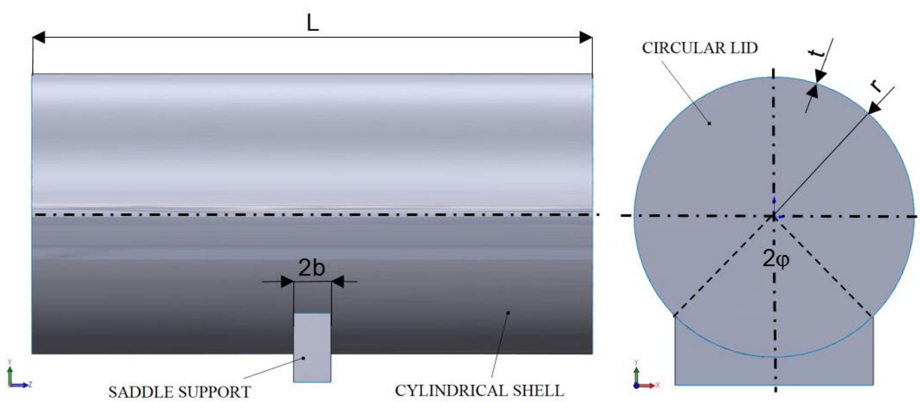

Fig. 2 Illustrative view of the computation model of a road tank with basic dimensions in [mm] for embracing angle of saddle support 2φ = 90°

Significant bending stresses induced by the saddle reaction are in the area between the circular lids and saddle support. This area is called the large shape discontinuity *a* [3] within which the bending stress is damped to an insignificant value. The specified shell length of the computational model guarantees that the stability analysis results in the saddle support area are not influenced by stiff circular lids. The large shape discontinuity for a cylindrical shell loaded with internal and external pressure can be expressed by the following equation [3]:

$$a = 2{,}5 \cdot \sqrt{r \cdot t} = 2{,}5 \cdot \sqrt{75 \cdot 0{,}55} = 16{,}1\,mm, \quad (1)$$

where *a* represents the distance of 16,1 mm in which the maximum stress drops to 4%, *r* and *t* are the parameters from **Tab. 1**. In the distance of 32,2 mm, the maximum stress drops to 4 ‰ as follows:

$$a = 5 \cdot \sqrt{r \cdot t} = 2{,}5 \cdot \sqrt{75 \cdot 0{,}55} = 32{,}2\ mm \cdot \quad (2)$$

In case of a cylindrical shell loaded with the saddle support reaction, a slower drop in stresses is expected. In spite of this, the results are supposed to be quite satisfactory, due to the sufficient shell length of 300 mm. It is, therefore, possible to expect relevant results, unnoticeably influenced by rigid circular lids.

2.2 Linear elastic bifurcation analysis (LBA)

The following chapter describes the linear buckling analysis (LBA), solving the static linear loss of stability of the cylindrical shell on the saddle support. The rough optimistic results were expected since the used LBA is only convenient for structures with quite predominant membrane stresses over the bending stresses. The main result is the lowest eigenvalue which represents the critical force F_{CR} for the unit load force F = 1. The corresponding eigenvector represents the shape of the deformation of the computational model at the moment of the loss of stability induced by the critical force F_{CR}. The physical sense has only the lowest eigenvalue and its corresponding eigenvector [12,13].

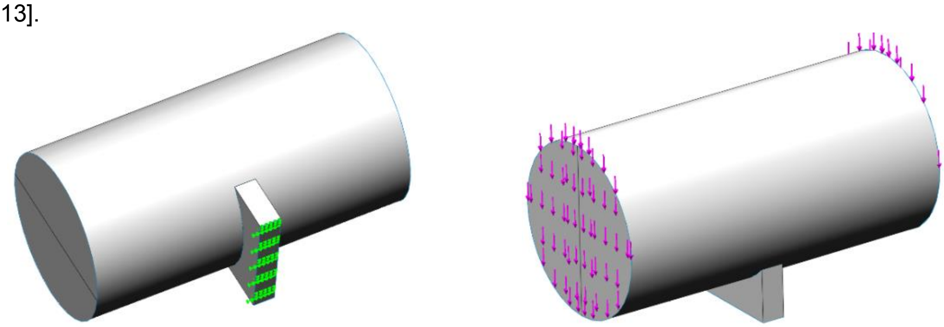

Fig. 3 Boundary condition (left), load (right)

The boundary conditions of the model and the calculated critical force for the various saddle support embracing angles are shown in **Fig. 3** and **Tab. 2**. In fact, significantly lower values of limit forces F_{LIM} obtained by geometric and material nonlinear analysis GMNA can be expected.

Tab. 2 Critical forces of considered saddle support embracing angles

Embracing angle of the saddle support		60°	90°	120°
F_{CR1}	[N]	7 576	17 082	29 029

2.3 Geometrically and materially nonlinear analysis (GMNA)

This chapter is devoted to the static geometrically and materially nonlinear analysis (GMNA). It results in a static carrying capacity of the shell represented by the limit vertical force F_{Slim}. The boundary conditions are the same as in the LBA in the previous chapter i.e., the saddle support is fixed at the base. The unit vertical force in the gravity direction is applied to both circular lids. The computational process has been controlled by the load curve arc increment process (Riks method) described in detail in literature [9]. The limit static forces for the considered embracing angles of the saddle support are shown in **Tab. 3**. The forces are compared with the significantly conservative forces $Q_{pl,Rd}$ obtained by the approximate analytical calculation [7]. It is evident, that the limit force of the approximate analytical solution for embracing angle 2φ = 120° is nearly 3 times lower than the limit force obtained by much more precise complete numerical analysis GMNA.

Tab. 3 Limit forces for considered embracing angles of the saddle support

Embracing angle of the saddle support		**60°**	**90°**	**120°**
F_{Slim}	[N]	2 452	4 630	9 866
$Q_{pl,Rd}$ [7]	[N]	1 695	2 543	3 390

For completeness, the following analytical formula to determine the approximate conservative limit force is used

$$Q_{pl,Rd} = 2 \cdot \left(0{,}975 \cdot \frac{s \cdot r \cdot t}{l_r} \cdot f_{y,d} \right), \tag{3}$$

where r, t and 2φ are defined in chapter 2.1 and other parts of formula (3) are shown below:

s - length of the saddle periphery in touch with the shell $(s = \pi \cdot r \cdot 2\varphi/180)$,
l_r - reference length $\left(l_r = r \cdot \sqrt{r \cdot t}\right)$ [7],
$f_{y,d}$ - yield strength.

2.4 Modal analysis of cylindrical shell welded to saddle support

The main objective of the modal analysis (MA) is to find the lowest significant eigenvalue in the form of a squared natural angular frequency ω^2. This is obtained by solving a homogeneous set of interdependent differential equations of the second order of the discrete FEM system (the generalized problem of eigenvalues and eigenvectors) [12, 13]

$$M \cdot \ddot{\Delta} + K \cdot \Delta = 0, \tag{4}$$

where **M** - mass matrix,
K - stiffness matrix,
$\ddot{\Delta}, \Delta$ - nodal acceleration vector, nodal displacement vector.

The subspace iteration method is used to solve the characteristic determinant

$$\det(K - \varpi^2 \cdot M) = 0. \tag{5}$$

Modal analysis has been performed for all three chosen to embrace angles of the saddle support 2φ = 60°/90°/120°. **Tab.4** lists the first four natural frequencies ($f_i = \omega_i/2\pi$) of the model for all considered embracing angles of saddle support.

Tab. 4 Summary of the natural angular frequency of all considered saddle support embracing angles

Embracing angle of the saddle support		**60°**	**90°**	**120°**
1.Mode	[Hz]	26,0	51,8	89,7
2.Mode	[Hz]	42,7	81,2	127,6
3.Mode	[Hz]	146,9	218,3	290,8
4.Mode	[Hz]	200,8	271,5	321,4

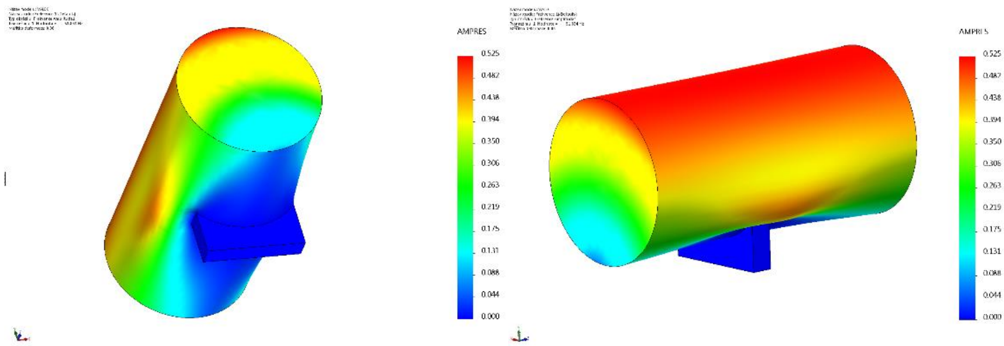

Fig. 4 The first nature mode (eigenvector) for saddle support embracing angle 2φ = 90°

For all the three cases of the embracing angle, the first natural frequency was significant since the corresponding modal mass m_1 reached about 60 % of the total mass of the model m_{TOT}. It means that 60% of the total mass vibrates in the first natural frequency with the first natural mode.

Based on the first natural frequencies, and further on the damping ratio $\xi = c/c_{CR} \approx 0{,}04$ valid for welded steel structures vibrating in the elastic-plastic limit state [14], the Rayleigh damping coefficients α_1, β_1 are determined. Due to the fact that the structure is damped at the first natural frequency at least, uniform damping at all frequencies $\xi = \xi_1 = 0{,}04$ is conservatively considered. Therefore, it is possible to write $\alpha = \alpha_1$, $\beta = \beta_1$. In the case of the cylindrical shell on the saddle support, damping has rather the numerical stabilization effect (it does not represent permanent vibration). For this reason, the Rayleigh coefficients for the angle 2φ = 90 ° may be used for all three embracing angles 2φ = 60°/90°/120°.

The procedure for the determination of the Rayleigh damping is given below. The damping matrix **C** can be simply expressed as a linear combination of the mass matrix ***M*** and stiffness matrix ***K*** [13,15]. It means that the damping forces are proportional to both the inertial forces and stiffness forces.

$$C = \alpha \mathrm{M} + \beta \mathrm{K} \tag{6}$$

Rayleigh's coefficients for saddle support embracing angle 2φ = 90° are:

$$\alpha = \xi \cdot \varpi_{01} = 0{,}04 \cdot 325{,}5 = 13{,}01 \sec^{-1}, \tag{7}$$

$$\beta = \xi / \varpi_{01} = 0{,}04 / 325{,}5 = 1{,}23 \cdot 10^{-4} \sec, \tag{8}$$

where the corresponding angular velocity is:

$$\varpi_{01} = 2 \cdot \pi \cdot f_{01} = 2 \cdot \pi \cdot 51{,}8 = 325{,}5\, rad \cdot \sec^{-1}. \tag{9}$$

The above-specified Rayleigh coefficients α and β are further used in the nonlinear dynamic analysis.

3 DYNAMIC ANALYSIS OF CYLINDRICAL SHELL ON SADDLE SUPPORT

The computational model dynamic nonlinear analysis is solved by a direct integration of the system of interdependent ordinary differential equations of the 2nd order of the discrete computational FEM model [13]:

$$\mathrm{M}\cdot\ddot{\Delta}+\mathrm{C}\cdot\dot{\Delta}+\mathrm{K}\cdot\Delta=F(t)\,, \tag{10}$$

where ***M*** - the mass matrix,
C - the damping matrix,
K - the stiffness matrix,
F(t) - time-dependent load vector,
$\ddot{\Delta}, \dot{\Delta}, \Delta$ - nodal acceleration/velocity/ displacement vector.

This is a dynamic problem with the consideration of geometrical and material nonlinearity. The Newmark integration method is used in the maximum time interval $t \in \langle 0 \div 0{,}001 \rangle$ *sec* with the integration step of approximately *t/50* (automatic selection of the integration step length) to calculate the response to the time variable load. The initial velocity v_0 = 1/2/3/4/5/10/15 m·sec^{-1} in the gravity direction is specified on both rigid circular lids. The saddle support is fixed at the base where the resulting time dependent vertical reaction is detected.

The load characteristic of **Fig. 5 to Fig. 8** expresses the time course of the resulting reaction for selected initial velocity v_0 = 1, 3, 10 m·sec^{-1} and embracing angle 2φ = 60°,90°,120°. The figures show that the course is higher and steeper with a higher load speed and vice versa. **Fig. 8** shows a deformed cylindrical shell with the saddle support of embracing angle 2φ = 60° in time 0, 0006 sec.

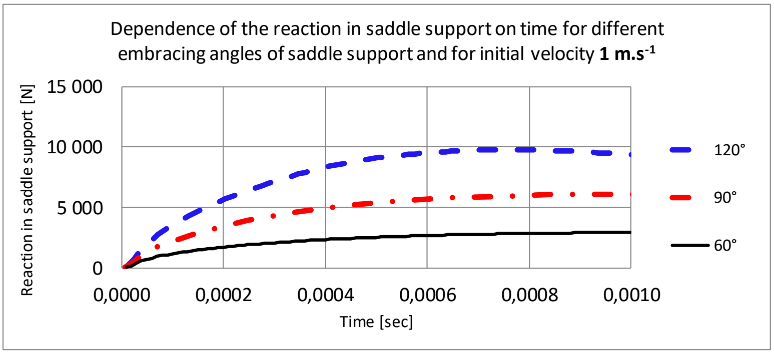

Fig. 5 Saddle support reaction for v_0 = 1 m.s^{-1}

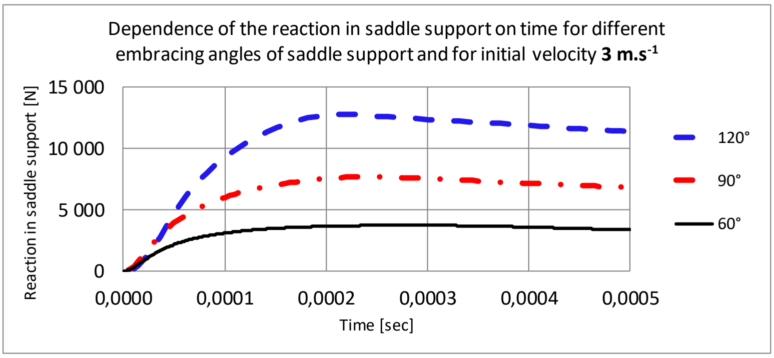

Fig. 6 Saddle support reaction for v_0 = 3 m.s^{-1}

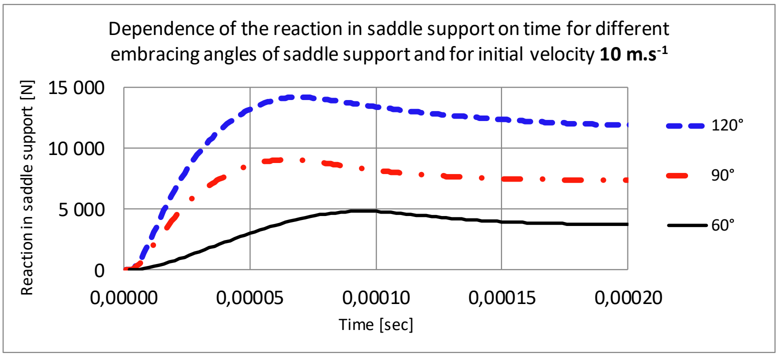

Fig. 7 Saddle support reaction for $v_0 = 10$ m.s^{-1}

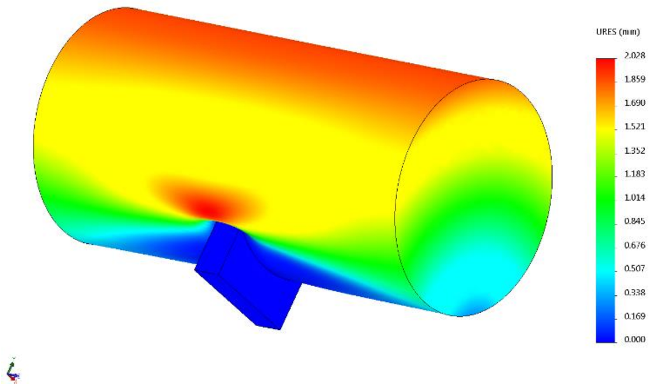

Fig. 8 Dynamic GMNA – total displacements for 2φ=60°

An important parameter of dynamic analysis is the magnitude of the maximum force F_{max}=-F_{Rmax} which leads to a stability snap-through of the saddle support into the cylindrical shell. These values are normalized to the static limit force F_{Dlim}/F_{Slim} and are built for all considered embracing angles and initial velocities into the diagram in **Fig. 9**. The higher carrying capacity of the dynamically loaded model is obvious. The computational model is more than two times more effective than a statically loaded model for embracing angle $2\varphi = 60°$ and initial velocity over 8 m·sec^{-1}.

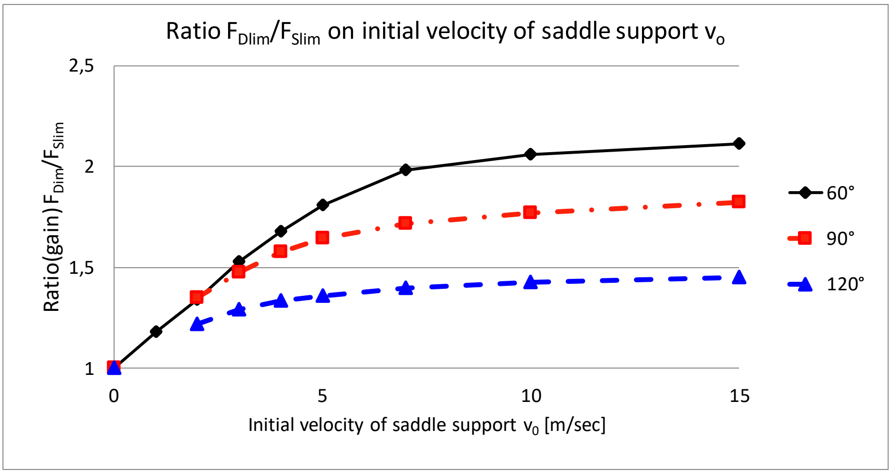

Fig. 9 Diagram of the ratio F_{Dlim}/F_{Slim} versus the initial velocity v_o

It is also evident that the saddle support does not snap-through into the shell for the initial velocity $v_0 = 1$ m.s^{-1} and the saddle support embracing angles $2\varphi = 90°$, $120°$. This is caused by the small initial momentum $p_0 = m.v_0$ of the computational model with the considered model weight of $m_{TOT} = 8{,}3$ kg.

4 CONCLUSION

Based on the results of the analysis, the behaviour of the cylindrical shell welded to the saddle support has been investigated. The limit loads leading to the stability snap-through of the saddle into the shell in the elastic-plastic field have been found. The dynamic analysis has been performed for various saddle support embracing angles $2\varphi = 60°/90°/120°$ and for various initial velocities of the cylindrical shell $v_0 = 1$, 2, 3, 4, 5, 10 and 15 m·sec^{-1}. It is evident that the limit force of the shell is increasing with the increasing initial velocity. The shell exhibits higher load carrying capacity at a dynamic load (stability resistance) than at a static load. In case of the saddle support embracing angle $2\varphi = 60°$ and the initial velocity $v_0 = 15$ m·sec^{-1}, the difference is more than twice as big. On the other hand, it is obvious that for a low initial velocity at a given weight of the structure, the stability snap-through does not occur. The shell oscillates around the established equilibrium position ($v_0 = 1$ m/sec, $2\varphi = 90°$ and $2\varphi = 120°$.

The work introduced in this article is the basis for a research in dynamic loading of a cylindrical shell firmly attached to a saddle support. In the next phase of the research, the attention will be drawn to the influence of initial manufacturing imperfections on the dynamic stability of this type of construction. The results will be verified by planned experiments on a reduced model at Education and Research Center in Transport (ERCT) of the Faculty of Transport Engineering, University Pardubice.

This research has been supported by the University of Pardubice in the scope of FRVŠ 1116/2011 project.

◆◆

Bibliography

[1] ČSN EN 13445-3 (2018). Unfired pressure vessels - Part 3: Design: 16.8 Vertical vessels on saddle supports (in Czech). Prague: Czech Standardization Agency, 2018.

[2] ČSN EN 1993-1-6 (2010) (in Czech): Eurocode 3: Design of steel structures - Part 6: Strength and stability of shell structures.

[3] ČSN 69 0010 (1991). Stationary pressure vessels. Design. Part 4-14: Spherical heads and covers without knuckle. Czechoslovak state norm, Prague. Federal Office for Standardization and Measurement, Prague.

[4] DIN 18800, part. 4 (1990) Structural steelwork. Analysis of safety against buckling of shells, German norm, English edition, Beuth Verlag GmbH, Berlin.

[5] AD-Merkblatter (2002) Technical Rules for Pressure Vessels, English edition, Carl Heymanns Verlag KG, Köln.

[6] ASME Boiler and Pressure Vessel Code, Section VIII, Pressure Vessels Division, 2. ED2010.

[7] ECCS 2013. Buckling of Steel Shells - European Design Recommendations, 5th Edition, Revised Second Impression, s. 385-397. ISBN 929147116X.

[8] Cistern TATRA PHOENIX. In: Serviscentrum Vysočina [online]. Jihlava: Kosovská 457/10, 586 01, Jihlava [cit. 2018-06-30]. Dostupné z https://www.scv-tatra.cz/x187-cisterna-tatra-phoenix

[9] PAŠČENKO, Petr, Petr TOMEK a Doubravka STŘEDOVÁ. Stability of thin-walled shell structures: Stability of spherical cap (in Czech). Pardubice: University Pardubice Studentská 95, Pardubice, 2013. ISBN 978-80-7395-697-4.

[10] FEM Computer program SIMULATION 2014 – Advanced Professional. SolidWorks Corporation

[11] ČSN EN 10025-2. *Výrobky válcované za tepla z konstrukčních ocelí: Část 2: Technické dodací podmínky pro nelegované konstrukčních oceli*. Praha: ČESKÝ NORMALIZAČNÍ INSTITUT, Praha, 2005.

[12] Wilson, E. L., Bath K. J. Numerical methods in Finite Element Analysis. 1976 by PRENTICE HALL, INC., Englewood Cliffs, New Jersey. ISBN 0-13-627190-1.

[13] Bitnar Z., Řeřicha P., Finite Element Method in Dynamics of Structures (in Czech). 1981 by SNTL, Praha.

[14] 2017 International Building Code 2017. Standard by International Code Council, 2017. ISBN(s): 978160983735.

[15] Alipour A., Zreian F., Study Rayleigh Damping in Structures; Uncertainties and Treatments. The 14th World Conference on Earthquake and Engineering. October 12-17, 2008, Beijing, China.